Early Warning of ionospheric disturbances for GNSS users

C. Borries and J. Berdermann
German Aerospace Center (DLR), Neustrelitz, Germany, mail: claudia.borries@dlr.de

Abstract: Temporal and spatial gradients in the ionosphere can cause major threats on communication and navigation satellite systems, because the propagation of transionospheric radio signals is influenced by the ionospheric electron content. Space weather events are often the source of strong ionospheric disturbances. Forecasting ionospheric perturbations related to space weather events is therefore a crucial task being of special interest for GNSS users.
The climatology of ionospheric storms seen in the Total Electron Content (TEC) over Europe as a response of the ionosphere towards Earth oriented space weather events is well known. It depends on season, elapsed time from event arrival, location and local time. However, the deviation of a single storm to the mean behavior can be large. A good correlation between strength of the ionospheric storm, i.e. the maximum deviation of the TEC to 27 day median, to solar wind or geomagnetic activity indices is hard to define. Hence forecasting TEC for disturbed conditions is a challenging task. However, the storm climatology and comprehensive correlation studies allow forecasting of the most probable TEC perturbation amplitude for the European region.
GNSS users are in need of information about arriving threads due to space weather events as early as possible. Therefore, an Early Warning message for GNSS users has been developed at the DLR within the FP7-Project AFFECTS. It provides information about Earth endangering space weather events to interested GNSS users up to two days before their arrival. Additional information are now added by a second warning message distributed thirty minutes before arrival at Earth giving more specific information like exact arrival time, forecasts of geomagnetic indices, approximate TEC perturbation and range error for the European region. An overview on the Early Warning for GNSS user service provided by DLR is presented in this paper.

BIOGRAPHIES

Claudia Borries has been working at the German Aerospace Center (DLR) in the Institute of Communications and Navigation since 2005. Main focus is the investigation of ionospheric disturbances incorporating disturbances of solar and geomagnetic origin as well as perturbations due to atmospheric influences from below. Furthermore she has scientific experience is in the field of inverse problems with sparsity constraints. In 2010 she completed her PhD at the Free University of Berlin, investigating the potential contribution of atmospheric waves to the atmosphere-ionosphere coupling. Today, she is involved in EU-FP7 and ESA projects related to space weather and essentially contributes to the development of the early warning system for GNSS users.

Jens Berdermann is head of the working group ionospheric effects and mitigation techniques at the DLR Institute of Communications and Navigation. He was/is involved as project lead for the DLR contributions in several national as well as ESA and EU projects (e.g. AFFECTS, ESPAS). His field of expertise is particle and space physics, space weather and data driven physical modelling of the ionosphere. Dr. Berdermann has published over 50 scientific papers in refereed journals and has presented numerous talks at national and international meetings.

1 INTRODUCTION

GNSS applications exist in various domains of the everyday life. In many cases their operability is a critical issue for financial efforts or even safety of life. The ionosphere is an important parameter influencing the operability of GNSS applications. Especially during disturbed conditions ionospheric

phenomena as e.g. scintillations and electron density gradients can limit the availability and accuracy of GNSS measurements. In most cases, severe ionospheric perturbations are related to solar transient events as e.g. coronal mass ejection, solar wind high speed streams and co-rotating interaction regions. Users and providers of communication and navigation services are in need of detailed and reliable information if their system will be affected and to which degree. In an initial step, an automated early warning message for GNSS users has been established within the EU FP7 project AFFECTS. It informs on a solar transient events potentially impacting the Earth atmosphere within the next 1-2 days. While the time ahead is pleasantly long, its uncertainty in time and actual occurrence is quite high. The user feedback revealed a missing link between the early warning and reliable information on concrete disturbances close to their occurrence. This reflects the need of dedicated forecasts of ionospheric disturbances and a comprehensive warning system.
Solar transient events coupling into the Earth magnetosphere usually transmit energy generating large perturbations in the high-latitude ionosphere and thermosphere what in turn results in strong plasma density variations. Dependent on local time and storm time, a propagation of the plasma perturbations towards lower latitudes is associated (Borries et al., 2013). Common ionospheric storm pattern have been derived in diverse ionospheric long term statistical analyses as well as case studies (Titheridge and Buonsanto, 1988; Jakowski et al., 1990; Borries et al., 2013; Förster and Jakowski, 2000; Borries et al., 2009; Liu et al., 2010; Lekshmi et al., 2011). However, the individual storm behaviour can deviate significantly from the common features.
Maps of the Total Electron Content (TEC) are a common tool for analysing and describing ionospheric conditions and deriving the range error. Based on the current TEC derivation from dual frequency signals from Global Navigation Satellite Systems (GNSS) and on a TEC background model (Jakowski et al., 2011), the SWACI service (http://swaciweb.dlr.de) provides routinely near real-time European and global TEC maps. This study will upgrade the characterisation of the impact of solar transient events on the Earth ionosphere in the European region based on the analyses of European TEC maps.

2 IONOSPHERIC WARNINGS

Accurately timed warnings can help essentially to mitigate threats from the ionosphere. Within the EU FP7-project AFFECTS (Advanced Forecast For Ensuring Communication Through Space, http://www.affects-fp7.eu) a fully operational early warning system for solar events has been developed. It contains a dedicated early warning message for GNSS users (http://swaciwebdevelop.dlr.de/early-warning-gnss/) distributed about one to two days before the potential arrival of a solar event (e.g. coronal mass ejection) at Earth. It comprises information on the expected arrival time at Earth, the predictions of the geomagnetic activity, the uncertainty of the arrival time and the event probability. The Early Warning Message for GNSS users can be seen as initial point for the development of a comprehensive ionospheric warning system for GNSS users with multi-level warnings ranging from long term predictions to real-time alerts. In this paper, we propose to develop a four level warning system (c.f. Fig. 1). Its first level will be covered by the AFFECTS early warning message for GNSS users. The second level will be called L1-Warning, named after the Earth-Sun liberation point (Lagrangian point L1), where satellites are orbiting at about 1.5 million kilometers from Earth, in the direct line between Sun and Earth. The Advanced Composition Explorer (ACE) satellite for example measures next to others solar wind and Interplanetary Magnetic Field (IMF) parameters which enable to estimate the arriving solar transient event approximately 30 minutes before arrival at Earth (dependent on solar wind speed). Geomagnetic and rough ionospheric predictions can be derived from these measurements. The third level will be based on the detection of ionospheric disturbances in the forecast, e.g. by analysing the deviation between quiet conditions and the forecast. Therefore, it will be called Forecast-Warning. The final level will be the near real-time Ionosperic-Alert, based on the detection of ionospheric perturbations in the current ionosphere, e.g. scintillations, TEC gradients and flares.
Within this paper, the development of the L1-Warning message will be discussed.

3 DATA AND MEASUREMENTS

TEC maps for the European region continuously produced since 1995 (Jakowski et al., 2002) are provided by the German Aerospace Center, DLR. The TEC is derived from groundbased GNSS measurements based on the first-order approximation of the TEC along the line of sight between satellite and receiver (slant TEC), which is proportional to the differential delay on the GNSS code and carrier phases. The measurements are mostly supplied by the international GNSS Service (IGS). After

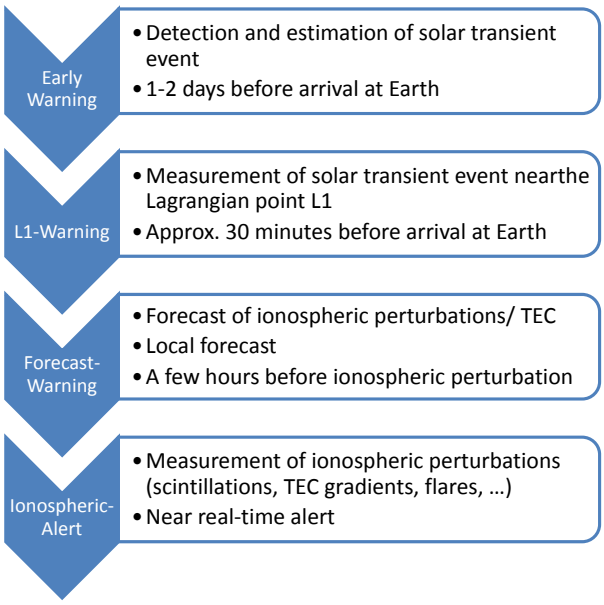

Figure 1: Four Level Ionospheric Warning System

using a special calibration technique, the slant TEC is mapped to the vertical by using a single layer approximation of the ionosphere at 400km height. The measurements are combined with a regional empirical TEC model (NTCM), developed at DLR, and mapped into a regular grid with $2.5^o \times 5^o$(latitude, longitude) grid size. The accuracy of the TEC maps is estimated with the order of 1 TECU (10^{16} electrons/m^2). Therefore it is suitable for monitoring large scale ionospheric perturbations.
In order to estimate TEC perturbations, relative differential TEC maps (subsequently referred to as ΔTEC) are derived as follows:

$$\Delta TEC = \frac{TEC - TEC_{med}}{TEC_{med}} \cdot 100\%. \quad (1)$$

TEC_{med} is the median TEC referring to a specific hour of the day within a 27 day window (related to the solar rotation period). The median TEC is calculated from the preceding 27 days, because the algorithm has to be applied in near real-time and the median should not contain the disturbance itself. Solar wind and IMF measurements near the Lagrangian point L1 are sampled onboard different satellites. One of them is the Advanced Composition Explorer (ACE) whose data is received amongst others at DLR in Neustrelitz. From its instruments we use in near real-time data of the Magnetic Field Experiment (MAG) and the Solar Wind Electron, Proton and Alpha Monitor (SWEPAM).

4 Analyses and Results

4.1 Ionospheric Storm Selection

In order to analyse features of ionospheric storms, we first have to define a selection of storm events. Since there hardly exist ionospheric parameters being appropriate as a storm indicator (due to the complexity of the ionospheric response to storm events), geomagnetic indices are usually applied for the definition of disturbed conditions. A common index is the Dst index, which we will use as storm indicator. We define storms as events with Dst below -50 nT. Additionally, the minimum in Dst of the preceding day has to be above -50 nT. This constraint is used to avoid the interference with preceding storm events in the process of deriving typical TEC storm features. The storm onset time is defined as the time of maximum Dst right before it starts decreasing.
By use of the storm definition above, we receive a list of 186 events within the time period between 1996 and 2013. Fig. 2 (left panels) presents a statistical overview on the occurrence of the selected storms. An increase in the occurrence during the solar maxima is clearly visible as well as the typical accumulation of storm events during equinoxes. The right panel of Fig. 2 illustrates the typical phases

of a geomagnetic storm to be observed with the Dst index. It starts with a quiet phase before the storm onset (stormtime$\leq$0), proceeds with the expansion phase with rapidly decreasing Dst right after the storm onset, followed by the peak of the substorm at minimum Dst and finally migrates into the recovery phase, when Dst is increasing slowly towards quiet values. The complete storm usually lasts more than three days. Most of the storms (62%) are moderate geomagnetic storms with Dst not decreasing below -100 nT, while 38% of the storms are classified as intense storms having a minimum in Dst below -100 nT (according to the categorisation of Gonzalez et al., 1994, and references therein). In our analyses, we divide into summer- (May to August), winter- (November to February) and equinox storms, as shown in Fig. 3 (lower panels), finding a similar number of storms in each season.

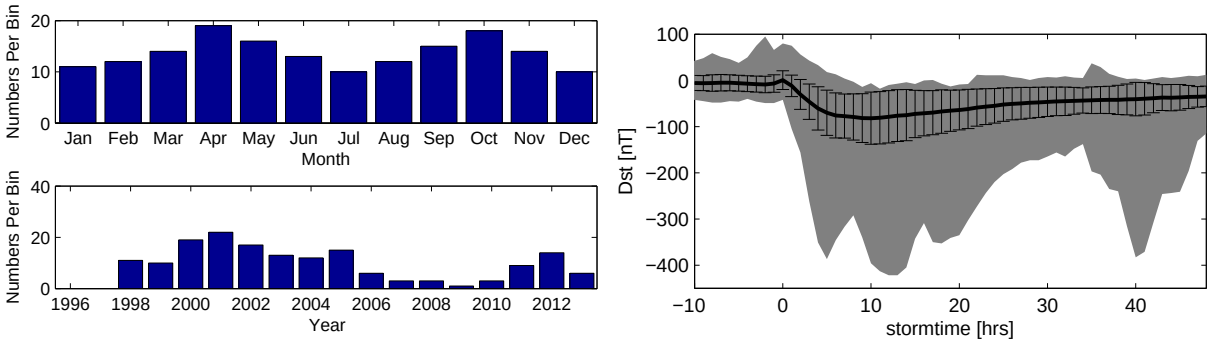

Figure 2: Left: Occurrence of the selected storms in dependence of month and year. Right: Dst index of the selected storms, where the black line shows the mean Dst. The error bars indicate one standard deviation and the grey shaded area encapsulates minimum and maximum values.

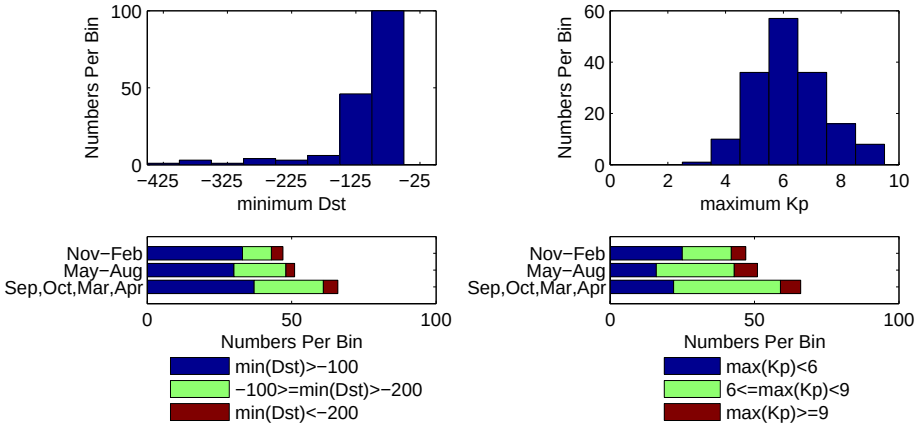

Figure 3: Characterization of the selected storms using Dst index (left panels) and Kp index (right panels). The storms are grouped in respect to season (winter, summer and equinox) and strength.

4.2 Characteristics of Ionospheric Storms

In order to extract typical TEC storm features for the European region, superposition analyses are applied on the ΔTEC maps. The superposition of all storms in one season results in quite complex storm features with a high deviation of the single storm, as shown e.g. in Borries et al. (2013). To achieve a more reliable image of storm features, we further separate the storms dependent on the storm onset time (0 to 6UT, 6 to 12 UT, 12 to 18UT and 18 to 0UT).
For each storm event plots are generated, containing the zonal mean ΔTEC data (computed from 0 to 20^{o}E) depending on time and latitude. The resulting superposition plots in Fig. 4 show the median value of the concerning time-latitudes plots. From left to right the panels show the features of storms with an onset during 0 to 6 UT, 6 to 12 UT (hereafter referred to as day storm), 12 to 18 UT and 18

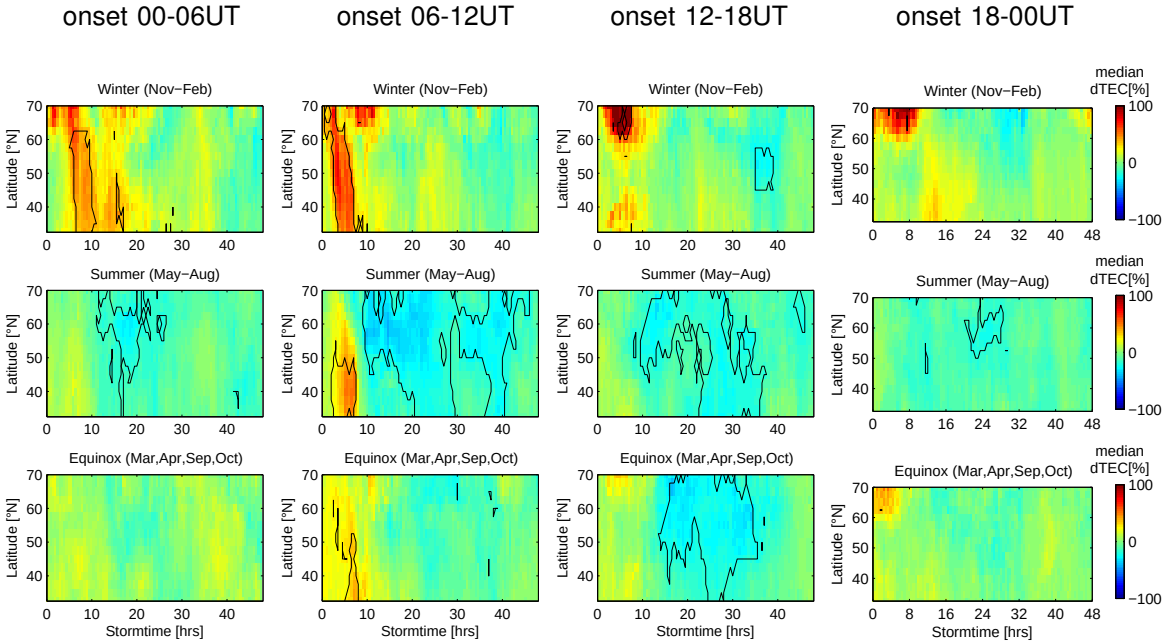

Figure 4: Median ΔTEC distribution depending on stormtime and season, derived by superposition of ΔTEC for selected storms. Stormtime zero refers to the storm onset time. Black lines encapsulate the sections, where the absolute median ΔTEC is larger than the standard deviation. The panels from left to right show the superposition of storms with an onset during 0 to 6 UT, 6 to 12 UT, 12 to 18 UT and 18 to 0 UT. From top to bottom panels show the superposition of winter, summer and equinoctial storms.

to 0 UT (hereafter referred to as night storm).

A clear difference between day and the night storms is visible. Only the day storms have clear positive storm features propagating southwards within the first ten hours after the storm onset. In winter, TEC enhancements start shortly after the storm onset in high latitudes. As the ionisation at the polar region is in winter generally quite low, small enhancements lead to large amplitudes in the ΔTEC. The night side ionisation enhancement during winter storms is usually associated with the tongue of ionisation, which describes a plasma transport due to an antisunward flow over the polar cap (Foster et al., 2005). In summer, the positive ΔTEC amplitude in polar regions is low and increases towards lower latitudes. Winter storms starting at 0 to 6 UT (before sunrise) first show for a few hours the typical perturbations in high latitudes before the TEC enhancement extends towards low latitudes (probably starting after sunrise). The median ΔTEC amplitude is strongest for summer storms with an onset time between 6 and 12 UT. Winter storms starting from 6 to 12 UT (around sunrise) typically develop immediately after the onset a positive storm feature propagating southwards. Source of these propagating positive storm features are neutral winds blowing in equatorial direction, modified by $E \times B$ plasma drifts caused by enhanced dawn-to-dusk electric fields (Jakowski et al., 1999; Prölss, 2006). The winds are uplifting the plasma along the field lines where the loss decreases, leading to a conservation of plasma. The preference of the equatorward propagation during daytime has also been found in (Baran et al., 2001; Borries et al., 2013; Förster and Jakowski, 2000; Ho et al., 1998; Jakowski et al., 1999; Lu et al., 2008; Immel and Mannucci, 2013). Based on the analyses shown in Fig. 4, the speed of the southward propagating positive storm feature can be approximated with 250 to 300 ms^{-1} on average. However, the front velocity of individual events might deviate a lot from the mean. E.g. in high latitudes such an ionisation front has been measured with about 110ms^{-1}(Mayer et al., 2008). Positive storm features have often been associated with Travelling Ionospheric Disturbances (TID, e.g. Borries et al., 2009; Ho et al., 1998). The TIDs are guided by thermospheric winds causing an effective uplifting of the plasma on the day side.

Summer storms show in general a clear negative phase, where a negative ΔTEC amplitude is generated around the peak storm time. It can also occur during winter but not as reliable as in summer. Negative storm features are generally well understood. They result from perturbations in the neutral gas composition (e.g. Prölss and Werner, 2002; Volland, 1983).

Finally, the differences between the features of summer and winter storms result from diverging global winds and composition. During equinoxes the thermospheric conditions change. Therefore, the equinoctial storm features are a mixture of summer and winter features.

4.3 Correlation to Solar Wind Parameters

Comprehensive correlation analyses between the ΔTEC amplitudes and solar wind and IMF parameters have already been shown in Borries et al. (2013). As only moderate and low correlations could be identified, the analyses are prolonged here.
The maximum ΔTEC amplitude estimated within the first 12 hours after the storm onset time is cross-correlated with the turning point of a solar wind or IMF parameter during that time, resulting in a normalized correlation coefficient and a confidence interval. This analyses has been executed for ΔTEC at each single latitude of the European map. Therefore, the plots in Figs. 5 and 6 show for each latitude the correlation coefficient (vertical bold line) and the confidence interval (grey shading). The correlation coefficient is indicated with a black line in case it is 95% significant. Otherwise it is grey.

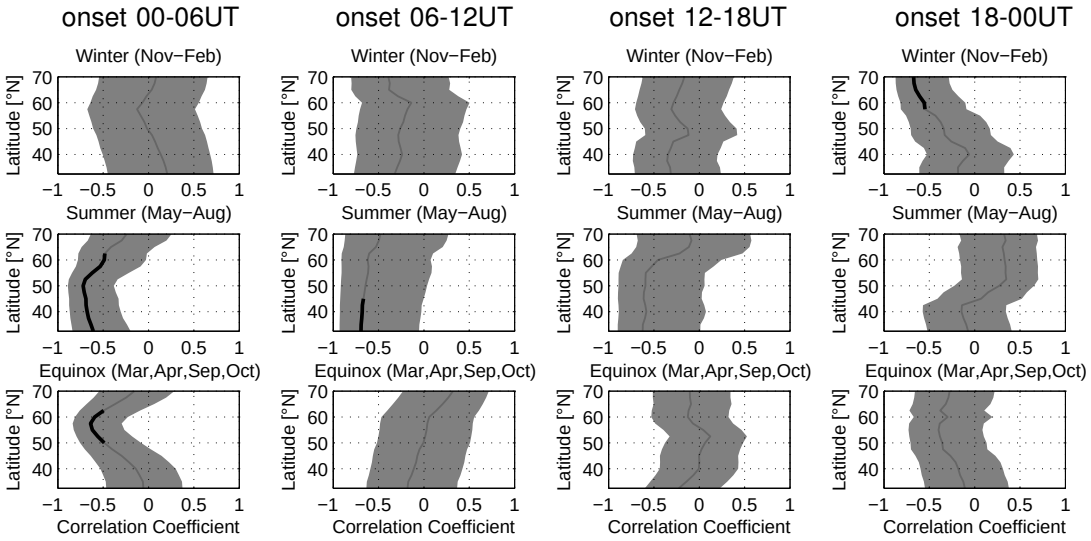

Figure 5: Correlation of maximum ΔTEC in the first 12 hours after the storm onset with minimum Bz (GSM coordinates measured at ACE-MAG). The normalized correlation coefficient (indicated on the X-axis) is calculated from the European zonal mean ΔTEC(0 to 20^{o}E) for each geographic latitude separately (indicated on the Y-axis). Black lines indicate significant correlation coefficients. The grey shading shows the 95% significance interval. The storms are grouped dependent on storm onset time (panels left to right: 0 to 6UT, 6 to 12UT, 12 to 18UT and 18 to 0UT) and season (panels top to bottom: winter, summer, equinox).

Correlation results are shown for the minimum value of the IMF Bz-component (Fig. 5) and the maximum value of the interplanetary electric convection field (Fig. 6). Bz is used a as a key parameter for the magnetosphere-ionosphere-system, because it is well known that persistent southward IMF produces strong dawn-to-dusk electric fields, increasing the geomagnetic activity (e.g. Gonzalez et al., 1994; Boudouridis et al., 2005). Additionally, we use the interplanetary electric convection field ($\vec{E} = -\vec{v} \times \vec{B}$) for our correlation studies. It depends on the strength of the IMF ($\vec{B}$) and the solar wind speed ($\vec{v}$). The variability of the interplanetary magnetic field triggers plasma instabilities in the tail of the magnetosphere and thus gives rise to magnetospheric storms (Volland, 1983). Furthermore, the electric field maps nearly undisturbed along the geomagnetic field lines to lower altitudes. In the lower thermosphere/ ionosphere (dynamo region) the electric fields are driving currents. Due to the dissipation of these currents the neutral gas in the dynamo region is heated via Joule heating. Irrotational winds with huge vertically-extended wind cells pervading the whole thermosphere develop due to this heat input (Volland, 1983). They are responsible e.g. for the plasma uplifting.
Generally, we still cannot prove very good correlation between TEC perturbation amplitudes and solar wind and IMF parameters. However, additional information can be derived from these analyses. E.g. the correlation to the IMF Bz component, which is observed during summer, is limited to day time. This describes the equatorwards propagating ionisation front. As there are in general hardly TEC

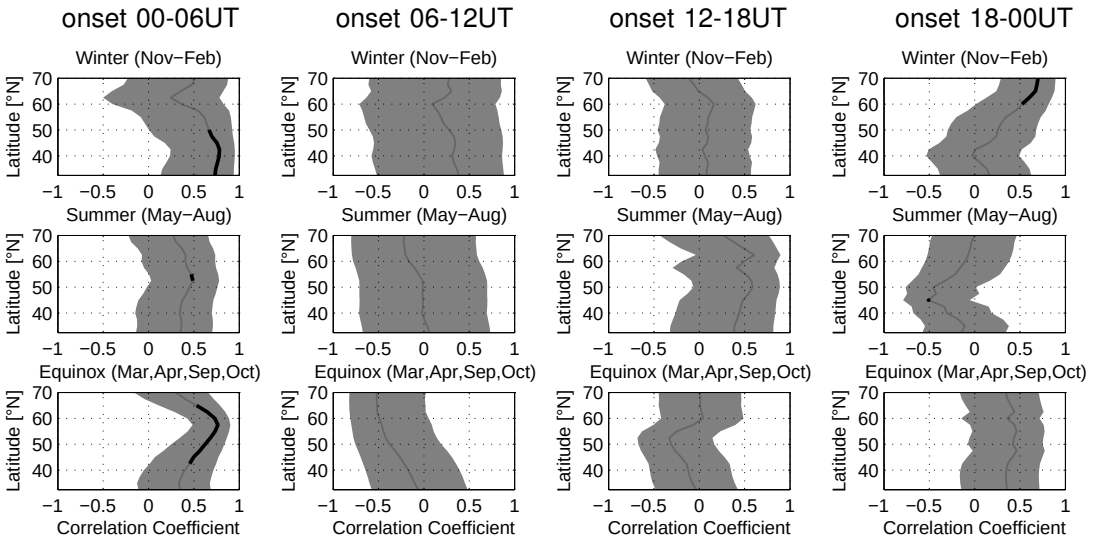

Figure 6: Correlation of maximum ΔTEC in the first 12 hours after the storm onset with maximum interplanetary electric convection field $\vec{E} = -\vec{v} \times \vec{B}$ (computed from ACE-MAG and ACE-SWEPAM measurements). The normalized correlation coefficient (indicated on the X-axis) is calculated from the European zonal mean ΔTEC(0 to 20°E) for each geographic latitude separately (indicated on the Y-axis). Black lines indicate significant correlation coefficients. The grey shading shows the 95% significance interval. The storms are grouped dependent on storm onset time (panels left to right: 0 to 6UT, 6 to 12UT, 12 to 18UT and 18 to 0UT) and season (panels top to bottom: winter, summer, equinox).

perturbations in summer in higher latitudes and during night (polar day), no correlation is expected there. Therefore, the results can be used well for describing positive summer storm features.
During winter, night time high latitude perturbations, caused by the tongue of ionisation, are well correlated with minimum Bz and maximum $|\vec{E}|$. The amplitudes of the winter day time positive storm features propagating equatorwards show good correlation with the maximum $|\vec{E}|$. Hence, the results hypothesize that winter storms are mainly driven by the convection electric field.
However, more sophisticated studies are necessary to investigate the origin and mechanisms of the single storm features.

5 DEVELOPMENT OF THE L1-WARNING MESSAGE

The L1-Warning will be based on ACE real-time measurements. It will be automatically issued directly after a storm detection using an automated detection algorithm. Therefore, ACE measurements have to exceed a critical value. Recently, the effective solar wind pressure p_{eff} has been introduced as a promising storm onset parameter (Borries et al., 2013), being derived from p and Bz measurements. Boudouridis et al. (2005) showed that southward IMF conditions combined with high solar wind dynamic pressure immediately after a pressure front impact lead to enhanced coupling between the solar wind and the terrestrial magnetosphere. Zhou and Tsurutani (2001) showed in a statistical study of 18 events that the auroral activity following a solar wind pressure enhancement was high for negative Bz, intermediate for near-zero Bz and low for positive Bz. p_{eff} is an easy approach combining Bz and p conditions in one number. Currently, the storm onset definition with $p_{eff} \geq 3$nPa as critical value is tested in operational use (http://swaciwebdevelop.dlr.de/solar-wind-data/).
A prototype version of the L1-Warning is shown in Fig. 7. It will contain a predicted ionosphere disturbance scale on top, which is based on a classification of the storm event. It will have three ionospheric conditions, I0 - Quiet (green), I1 - Disturbed (yellow), I2 - Storm (red). The following information in the L1-Warning message is the predicted start time, which indicates the time the solar transient event will arrive at Earth and potentially start transferring energy into the high latitude magnetosphere-ionosphere. Dependent on latitude, storm time and local time, the maximal ionospheric disturbances can occur hours later (c.f. Sec. 4.2). Next, the L1-Warning message contains information on the predicted ionosphere and predicted geomagnetic activity, based on the correlation between ACE measurements and ionospheric and geomagnetic disturbances. Following to the current correlation results presented in Sec. 4.3, most positive storm features can be estimated for selected storm events

Predicted ionosphere disturbance scale:	I1 - Disturbed	
Predicted start time:	08. July 2013 01:36 UTC This is the time of the solar transient event arriving at Earth. The maximum ionospheric and geomagnetic disturbances can occur up to 24 hours after the predicted start time.	
Predicted Ionosphere:	predicted DIX:	not specified
	predicted Maximum TEC (>60°N):	not specified
	predicted Maximum TEC (40°N to 60°N):	not specified
	predicted Maximum TEC (>60°N):	not specified
	Forecast TEC map:	Forecast TEC maps up to 24 hours in advance. The forecast is based on a perturbation TEC model, predicting the most probable development of the ionospheric storm condition.
	Current TEC map:	Current and one hour forecasted TEC maps, provided by SWACI.
Predicted geomagnetic activity:	predicted maximum Kp: not specified predicted minimum Dst: 0	
Expected Hazards:	Impacts on high frequency (HF) radio propagation expected. Influence on positioning and navigation is possible.	
Probability of incidence:	not specified	

Related solar transient event:

event type: not specified

event ID: 2.0

update no: 0

Source: SWACI Service at German Aerospace Center - DLR

Issued: 2013-07-08T02:00:00

Figure 7: Prototype layout of the L1-Warning Message.

and regions and events with low probability of TEC enhancement can be identified. What follows at the end of the message is a description of the expected hazards and an assessment of the probability of the event.

The initial L1-Warning for each potential ionospheric storm will be disseminated via the SWACI service (http://swaciwebdevelop.dlr.de/early-warning-gnss/) and subscribed users will receive it via email. As the storm conditions can emphasize after the initial storm onset detection, the predicted geomagnetic and ionospheric parameters might have to be adjusted during the storm progress. In this case an updated message will be issued on the website.

Using the L1-Warning one has to be aware of its constraints. The first constraint is obvious, regarding the analyses shown in section 4.3. As we can currently only find moderate correlation between solar wind parameters and TEC disturbances, the reliability of maximum TEC prediction is also only moderate. Second, the L1-Warning depends on the availability of the storm onset indicator p_{eff} based on ACE-MAG and ACE-SWEPAM instrument measurements onboard ACE. No continuous data can be guaranteed. Therefore, it is possible that single storm events cannot be detected with this algorithm. One backup is the usage of a second storm onset definition based on Dst forecast. Dst, which is well correlated with Bz, can be estimated using only ACE-MAG measurements (Parnowski and Polonska, 2012; Parnowski et al., 2014). Usually, ACE-MAG is the more reliable instrument of both. In any case,

the potential lack of single L1-Warning messages is supposed to be compensated by the Forecast-Warning and the near real-time Ionospheric-Alert. These will depend on ionospheric observations (mainly TEC), which usually have high performance and reliability.

6 CONCLUSION

The need of communication and navigations users and providers for early and precise warnings on forthcoming and current ionospheric disturbances is addressed with the development of a four-level Ionospheric Warning System. It comprises an Early Warning Message, 1-2 days before the potential arrival of a solar transient event at Earth, a L1-Warning Message, about 30 minutes before the actual arrival of a solar transient at Earth, a Forcast Warning Message, based on ionospheric storm models and predictions and an near real-time Ionospheric Alert, based on near real-time estimation of ionospheric disturbances.

Having established the automated Early Warning Message for GNSS users within the EU FP7 project AFFECTS, a prototype of the automated L1-Warning Message has now been implemented (http://swaciwebdevelop.dlr.de/early-warning-gnss/). It informs service providers and users about potential ionospheric disturbances short hand before the onset of an ionospheric storm. Maximum TEC perturbations are provided based on extensive storm analyses.

However, the ionospheric response to solar transient events is quite complex. Therefore, the analyses shown here have to be seen as pre studies which are supposed to be strengthened in near future in order to improve the understanding of ionospheric storms and to increase the reliability of the TEC predictions for storm conditions.

ACKNOWLEDGMENT

The authors acknowledge the support by the EU within the FP7 projects AFFECTS (grant agreement no. 263506, www.affects-fp7.eu). Furthermore, we would like to thank the ACE Science Center for the providing ACE data through their data server at http://www.srl.caltech.edu/ACE/ASC. Kp indices have been kindly provided by the NOAA Satellite and Information Service through their web page http://www.nesdis.noaa.gov. World Data Center for Geomagnetism, Kyoto, has been kindly providing the Dst index.

REFERENCES

Baran, L., Ephishov, I., and Shagimuratov, I. (2001). Ionospheric Total Electron Content Behaviour During November 1997 Storm. *Phys. Chem. Earth (C)*, 26(5):341–345.

Borries, C., Berdermann, J., Jakowski, N., Hoque, M., and Bothmer, V. (2013). Preparation of an advanced TEC forecast based on the statistical analysis of historical ionospheric storms. In *Proceedings of the 4th International Colloquium on Scientific and Fundamental Aspects of the Galileo Programme (ESA Publication WPP-335)*.

Borries, C., Jakowski, N., and Wilken, V. (2009). Storm induced large scale TIDs observed in GPS derived TEC. *Annales Geophysicae*, 27(4):1605–1612.

Boudouridis, A., Zesta, E., Lyons, L. R., Anderson, P. C., and Lummerzheim, D. (2005). Enhanced solar wind geoeffectiveness after a sudden increase in dynamic pressure during southward imf orientation. *Journal of Geophysical Research: Space Physics*, 110(A5):A05214.

Förster, M. and Jakowski, N. (2000). Geomagnetic Storm Effects on the Topside Ionosphere and Plasmasphere: A Compact Tutorial and New Results. *Surveys in Geophysics*, 21(1):47–87.

Foster, J. C., Coster, A. J., Erickson, P. J., Holt, J. M., Lind, F. D., Rideout, W., McCready, M., van Eyken, A., Barnes, R. J., Greenwald, R. A., and Rich, F. J. (2005). Multiradar observations of the polar tongue of ionization. *Journal of Geophysical Research: Space Physics*, 110(A9):A09S31.

Gonzalez, W. D., Joselyn, J. A., Kamide, Y., Kroehl, H. W., Rostoker, G., Tsurutani, B. T., and Vasyliunas, V. M. (1994). What is a geomagnetic storm? *Journal of Geophysical Research: Space Physics*, 99(A4):5771–5792.

Ho, C. M., Mannucci, A. J., Sparks, L., Pi, X., Lindqwister, U. J., Wilson, B. D., Iijima, B. A., and Reyes, M. J. (1998). Ionospheric total electron content perturbations monitored by the gps global network during two northern hemisphere winter storms. *Journal of Geophysical Research: Space Physics*, 103(A11):26409–26420.

Immel, T. J. and Mannucci, A. J. (2013). Ionospheric redistribution during geomagnetic storms. *Journal of Geophysical Research: Space Physics*, 118(12):7928–7939.

Jakowski, N., Heise, S., Wehrenpfennig, A., Schlüter, S., and Reimer, R. (2002). GPS/GLONASS-based TEC measurements as a contributor for space weather forecast. *Journal of Atmospheric and Solar-Terrestrial Physics*, 64(5-6):729–735.

Jakowski, N., Hoque, M. M., and Mayer, C. (2011). A new global TEC model for estimating transionospheric radio wave propagation errors. *Journal of Geodesy*, 85(12):965–974.

Jakowski, N., Putz, E., and Spalla, P. (1990). Ionospheric Storm Characteristics Deduced from Satellite Radio Beacon Obervations at Three European Stations. *Annales Geophysicae*, 8(5):343–352.

Jakowski, N., Schlüter, S., and Sardon, E. (1999). Total electron content of the ionosphere during the geomagnetic storm on 10 January 1997. *Journal of Atmospheric and Solar-Terrestrial Physics*, 61(3-4):299–307.

Lekshmi, V., Balan, N., Ram, S. T., and Liu, J. Y. (2011). Statistics of geomagnetic storms and ionospheric storms at low and mid latitudes in two solar cycles. *J. Geophys. Res.*, 116:A11328.

Liu, J., Zhao, B., and Liu, L. (2010). Time delay and duration of ionospheric total electron content responses to geomagnetic disturbances. *Annales Geophysicae*, 28(3):795–805.

Lu, G., Goncharenko, L. P., Richmond, A. D., Roble, R. G., and Aponte, N. (2008). A dayside ionospheric positive storm phase driven by neutral winds. *J. Geophys. Res.*, 113:A08304.

Mayer, C., Jakowski, N., Borries, C., Pannowitsch, T., and Belabbas, B. (2008). Extreme ionospheric conditions over Europe observed during the last solar cycle. In *Proceedings of the 4th ESA Workshop on Satellite Navigation User Equipment Technologies*.

Parnowski, A. and Polonska, A. (2012). Regression modelling of the interaction between the solar wind and the terrestrial magnetosphere. *Journal of Physical Studies*, 16(1/2):1002.

Parnowski, A., Semeniv, O., Polonska, A., Malisse, V., and Verbeeck, C. (2014). Geomagnetic forecast tool. *Journal of Space Weather and Space Climate*, submitted.

Prölss, G. and Werner, S. (2002). Vibrationally excited nitrogen and oxygen and the origin of negative ionospheric storms. *J. Geophys. Res.*, 107:1016, 6 PP.

Prölss, G. W. (2006). Ionospheric F-region Storms: Unsolved Problems. In *Characterising the Ionosphere*, Meeting Proceedings RTO-MP-IST-056, pages 10–1 – 10–20.

Titheridge, J. E. and Buonsanto, M. J. (1988). A comparison of Northern and Southern Hemisphere TEC storm behaviour. *Journal of Atmospheric and Terrestrial Physics*, 50:763–780.

Volland, H. (1983). Dynamics of the disturbed ionosphere. *Space Science Reviews*, 34:327–335.

Zhou, X. and Tsurutani, B. T. (2001). Interplanetary shock triggering of nightside geomagnetic activity: Substorms, pseudobreakups, and quiescent events. *Journal of Geophysical Research: Space Physics*, 106(A9):18957–18967.